BMC Immunology

RESEARCH

Open Access

mTORC2 is crucial for regulating the recombinant *Mycobacterium tuberculosis* CFP-10 protein-induced phagocytosis in macrophages

Xian-Hui Huang[1†], Yu Wang[1†], Liu-Ying Wu[1,4†], Ye-Lin Jiang[1†], Ling-Jie Ma[1], Xiao-Feng Shi[1], Xing Wang[1], Meng-Meng Zheng[3], Lu Tang[5*], Yong-Liang Lou[1,2*] and Dan-Li Xie[1,2*]

Abstract

Mycobacterium tuberculosis (*M. tuberculosis*, *Mtb*) is a pathogenic bacterial species in the family Mycobacteriaceae and the causative agent of most cases of tuberculosis. Macrophages play essential roles in defense against invading pathogens, including *M. tuberculosis*. The study of *M. tuberculosis*-associated antigens is one of the hotspots of current research. The secreted proteins of *M. tuberculosis*, including early secretory antigen target 6 (ESTA6) and culture filtrate protein 10 (CFP-10), are crucial for the immunological diagnosis of tuberculosis. However, the relationship of CFP-10 alone with macrophages is still not well understood. In the present study, we report that the purified recombinant protein CFP-10 (rCFP-10) significantly enhanced the phagocytic capacity of murine macrophages. rCFP-10 induces both TNF-α and IL-6 production. Additionally, RNASeq analysis revealed that rCFP10 triggers multiple pathways involved with macrophage activation. Interestingly, neither mitochondrial reactive oxygen species nor lysosomal content had a significant difference treated with rCFP-10 in macrophages. Moreover, inhibition of the mammalian target of rapamycin (mTOR) activity was shown to significantly reverse the rCFP10-induced phagocytosis, various genes involved in lysosome acidification and TLR signaling. These findings highlight that the CFP-10 plays an essential role in the invasion of macrophages by *M. tuberculosis*, which is partly regulated by the mTORC2 signal pathway.

Keywords *Mycobacterium tuberculosis*, Culture filtrate protein 10, Mammalian target of Rapamycin complex 2, Phagocytosis

[†]Xian-Hui Huang, Yu Wang, Liu-Ying Wu and Ye-Lin Jiang contributed equally to this work.

*Correspondence:
Dan-Li Xie
xiedl001@wmu.edu.cn
Yong-Liang Lou
lyl@wmu.edu.cn
Lu Tang
tanglu9106@foxmail.com

[1]The School of Laboratory Medicine & Life Sciences, Key Laboratory of Laboratory Medicine, Wenzhou Medical University, Ministry of Education of China, Wenzhou, Zhejiang 325035, China
[2]Wenzhou Key Laboratory of Sanitary Microbiology, Wenzhou, Zhejiang 325035, China
[3]Scientific Research Center, Wenzhou Medical University, Wenzhou, Zhejiang 325035, China
[4]Department of Laboratory Medicine, Lishui Municipal Central Hospital, Lishui, Zhejiang 323000, China
[5]Department of Urology, Chinese PLA General Hospital, Beijing 100853, China

Introduction

Mycobacterium tuberculosis (*M. tuberculosis*, *Mtb*) is a pathogenic bacterial species in the family Mycobacteriaceae and the causative agent of most cases of tuberculosis, which infects dendritic cells (DCs), monocytes (Mons), macrophages (Mϕ), and alveolar epithelial cells [1, 2]. The *Mtb* genome encodes five type VII secretion systems, including early secretory antigen target 6 (ESAT-6) secretion system-1 (ESX-1), ESX-2, ESX-3, ESX-4, and ESX-5. The ESX-1 is one of the most critical pathways in the pathogenesis of *Mtb* [3, 4]. ESX-1primarily encodes two potent T cell antigens, ESAT-6, and culture filtrate protein 10 (CFP-10), located within the RD1 region of pathogenic mycobacteria [5]. Both human and animal immune systems can recognize CFP-10 in the early stages of the disease, stimulating a robust immune response in the host [6, 7]. Several previous studies have found CFP-10 to be an antigenic protein for diagnosing tuberculosis based on the immunological aspects of CFP-10. However, the relationship between CFP-10 and macrophages in the pathogenesis of *Mtb* is still unclear.

The intracellular pathogen *Mtb* causes long-term infection in humans that mainly attacks macrophages and can escape the immune system through various mechanisms [8]. *Mtb* can escape from the phagosome and survive in the cytoplasm of macrophages [9]. Many mycobacterial virulence proteins have been previously found to interfere with phagosome-lysosome fusion in macrophages [10–12]. Furthermore, the macrophage proteome and the *Mtb* proteome microarray interaction revealed positive signals for more than 500 *Mtb* proteins [13]. Alternatively, *Mtb* replication, which subsequently spreads to neighboring cells, is facilitated by escape from phagosomes, resulting in damage to the plasma membrane through the ESX-1 protein [14]. Based on a range of model systems in vitro and in vivo, the RD1 gene encodes a region of the tuberculosis genome that codes for a type VII secretion system involved in the organism's virulence [15]. In addition, as a consequence of *Mtb* infection, the metabolism of macrophages is also altered, and their phenotype changes to one that is more pro-inflammatory [16].

The mammalian target of rapamycin (mTOR) is a serine/threonine protease of 289 kDa, a member of a family of kinases related to phosphatidyl inositol 3-kinase (PI3 K). In mammalian cells, mTOR is present in mTORC1 and mTORC2, which control specific innate immune cell effector functions, including metabolism, phagocytosis, and cytokine production [17, 18]. The mTOR signaling pathway is activated during infection and plays an important role against *Mtb*. In addition to its direct effect on host defense, mTOR can also play a role as a regulator of cytokine production and chemokine receptor activation.

In this work, we observed that purified rCFP10 could induce both TNF-α and IL-6 production of murine macrophages, as well as enhanced the phagocytic capacity of murine macrophages. These processes could be partly regulated by the mTORC2 signal pathway. But rCFP-10 did not affect mitochondrial reactive oxygen species or lysosomal content in macrophages. These results provide a strategy for improving the immune response to *Mtb* and effective treatment of tuberculosis.

Results

Cytotoxicity of the rCFP-10

The SDS-PAGE analysis of purified rCFP-10 protein showed only a single protein band, and no other spurious bands were observed (Fig. 1A). Purified rCFP-10 proteins were found to have low levels of endotoxin (Supplement Fig. 1, lane 1). However, after the Endotoxin Removal Kit treatment, the endotoxin of rCFP-10 was abolished (Supplement Fig. 1, lane 2). Considering the potential cytotoxicity, we first evaluated the cytotoxicity of rCFP-10 to murine Bone marrow derived macrophage (BMMϕ) and murine macrophage J774A.1 cells by CCK8 assay. Based on the results of the CCK8 assay, nearly 100% of the J774A.1 cells were viable under rCFP-10 treatment (Fig. 1B). BMMϕ also shows similar findings (Fig. 1C). These results indicated that the concentration of rCFP-10 that we tested in the studies showed no significant cytotoxicity.

Modulation of macrophage activation by rCFP-10

To understand the relationship between the rCFP-10 and macrophages. We performed RNA-seq and transcriptomic analysis both in J774A.1 cells and BMMϕs with and without the rCFP-10 treatment. RNA-seq analysis revealed substantial changes to the transcriptome of macrophages. The KEGG pathway enrichment analysis demonstrated that the top pathways involved in TNF signaling, NF-kappa B signaling (NF-κB), and NOD-like receptor (NLR) signaling were over-represented following rCFP-10 treatment (Fig. 2A), we were drawn to the up-regulation of PI3 K-Akt signaling and mTOR signaling. We then proceeded to analyze the differentially expressed genes using the hallmark gene sets from the Molecular Signatures Database (MSigDB) and *GO Term*, which revealed a substantial up-regulation of genes involved in the inflammatory response process and phagocytic cup (Fig. 2B, C). Our results indicated that the rCFP-10 trigger the inflammatory response and phagocytosis of macrophages that the activation of PI3 K-Akt and mTOR signaling pathways may accompany.

rCFP-10 enhances macrophage phagocytosis in vitro

Previous studies have shown that TNF-α may contribute to triggering protective immune responses in *Mtb*

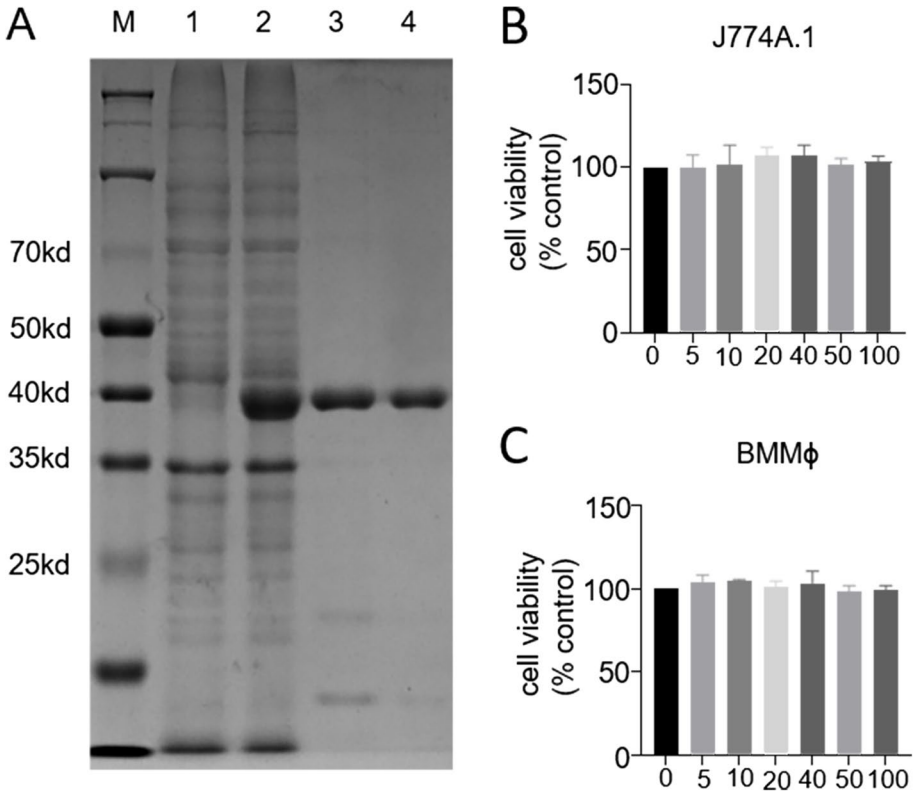

Fig. 1 The purified recombinant CFP-10 protein showed low levels of endotoxin which has no impact on the viability of Macrophages. **A** Purified rCFP-10 protein was subjected to SDS-PAGE. Lane M = protein molecular weight standards; lane 1 = uninduced recombinant CFP-10 strain; lane 2 = induction of recombinant CFP-10 strain; lane 3 = purified recombinant CFP-10 protein by His-tag Protein Purification Kit; lane 4 = purified recombinant CFP-10 protein by Ionic exchange. **B**, **C** The Cell Counting Kit-8 allows for the detection of viability in rCFP10-treated macrophages. The data shown are representative of a minimum of three experiments. *: $P < 0.05$; **: $P < 0.01$; ***: $P < 0.001$ was determined by Student *t*-test

infection [19], and IL-6 can enhance the host immunity against *Mtb* infection by promoting the production of IFN-γ [20]. We found that the rCFP-10 treated macrophages exhibited up-regulation of TNF-α and IL-6 production (Fig. 3A). And RNA-seq and transcriptomic analysis allow us to understand that the rCFP-10 triggers macrophage phagocytosis (Fig. 2B, C). Flow cytometry examined in vitro macrophage phagocytosis with the effect of rCFP-10. As shown in Fig. 3B, rCFP-10 promoted macrophage phagocytosis under different durations in a time-dependent manner. Pathogens activate macrophages to elaborate proinflammatory cytokines production and bactericidal molecules, such as ROS [21]. In addition, macrophages recruit mitochondrial ROS to the vicinity of phagocytic lysosomes to defend against invading bacteria [22, 23]. In contrast, we observed that mitochondrial ROS and lysosomal content levels did not differ significantly with or without rCFP-10 treatment (Fig. 3C, D). These findings suggested that the rCFP-10 contributes to *Mtb* hijacking macrophages against phagocytosis and may allow intracellular *Mtb* survival.

mTORC2 activity was crucial for rCFP10-induced macrophage defense responses

Previous studies have reported that the mTOR signaling pathway was important against *Mtb* infection [24]. In contrast, the consequence of mTOR signaling to the rCFP10-induced phagocytosis of macrophages remains unknown. We determined the mTOR signaling in macrophages after rCFP-10 treatment. The rCFP10-treated macrophages exhibited elevated mTOR, S6K, and S6 phosphorylation (Fig. 4A, B), indicating that rCFP-10 might activate mTOR signaling in vitro. The effect of the mTOR signal pathway on macrophage phagocytosis is well known [25, 26]. We then determined whether mTOR activity affected the phagocytosis capacity of macrophages. Interestingly, we found no significant difference in the percentage of phagocytosis-positive macrophages between rCFP10 stimulated J774A.1 cells with or without rapamycin (mTORC1 inhibitor) treatment (Fig. 4C-E). Similar results were observed in rCFP-10 with rapamycin-treated BMMϕ (Fig. 4C-E). In mammalian cells, mTOR is known to exist in two complexes: mTORC1 and mTORC2 [27]. In addition, we tested the percentage of phagocytosis-positive macrophages, which were treated with rCFP-10 with Torin1 (inhibitor

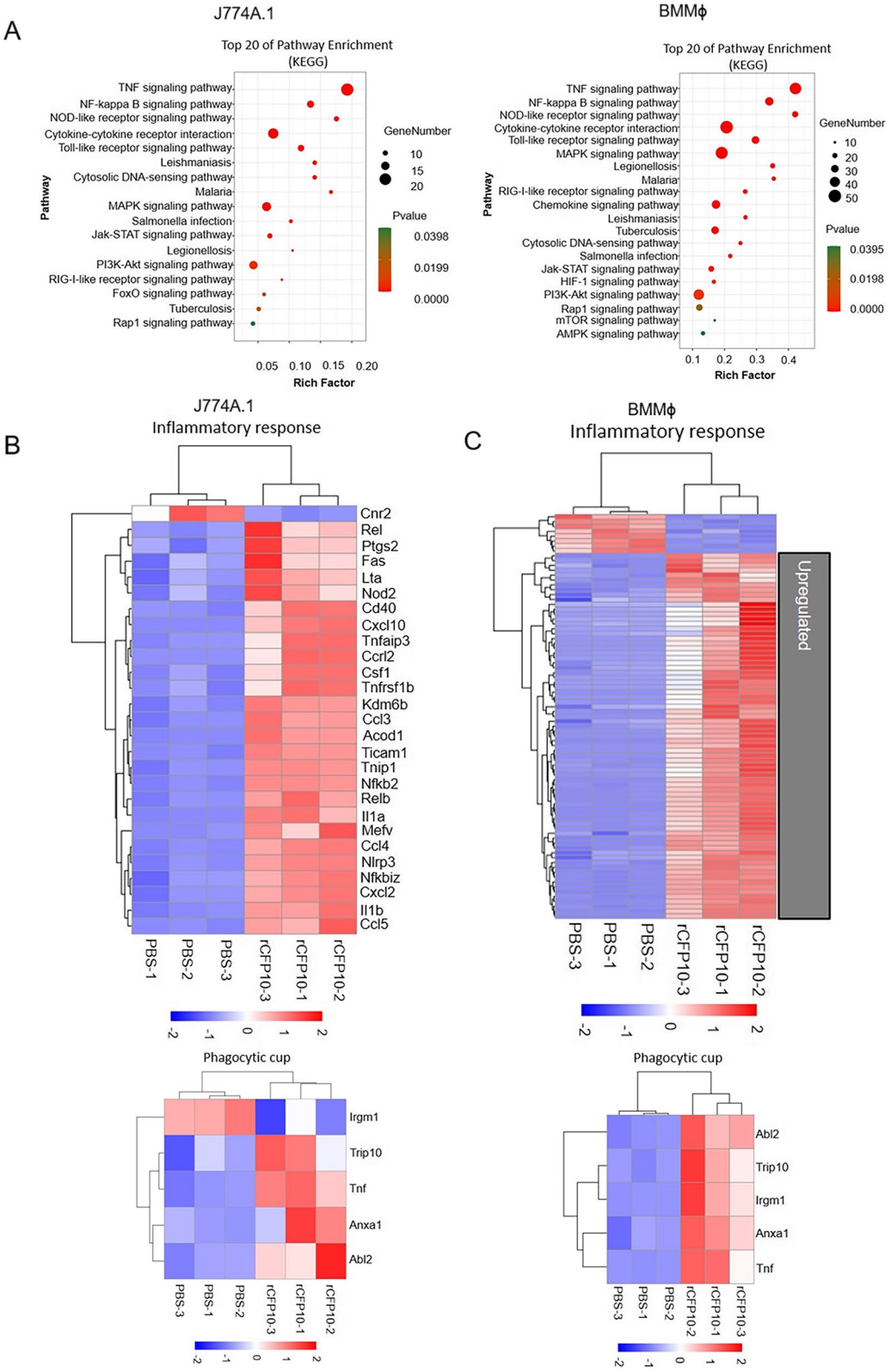

Fig. 2 The rCFP-10 was shown to induce several cellular biological events in macrophages. **A** Analysis of the KEGG pathway of the genes 1 h following 100 μg/ml of rCFP-10 treatment. **B**, **C** Heatmap of transcriptional profiles of J774A.1 cells and BMMϕ with or without rCFP-10 treatment (PBS: $n = 3$; rCFP-10: $n = 3$). Gene expressions are presented as log2 fluorescence intensity centered and scaled (blue and red keys) grouped according to the product functions. **B** The inflammatory response and phagocytic cup expressed in the J774A.1 cell. **C** Inflammatory response and phagocytic cup expressed in BMMϕ

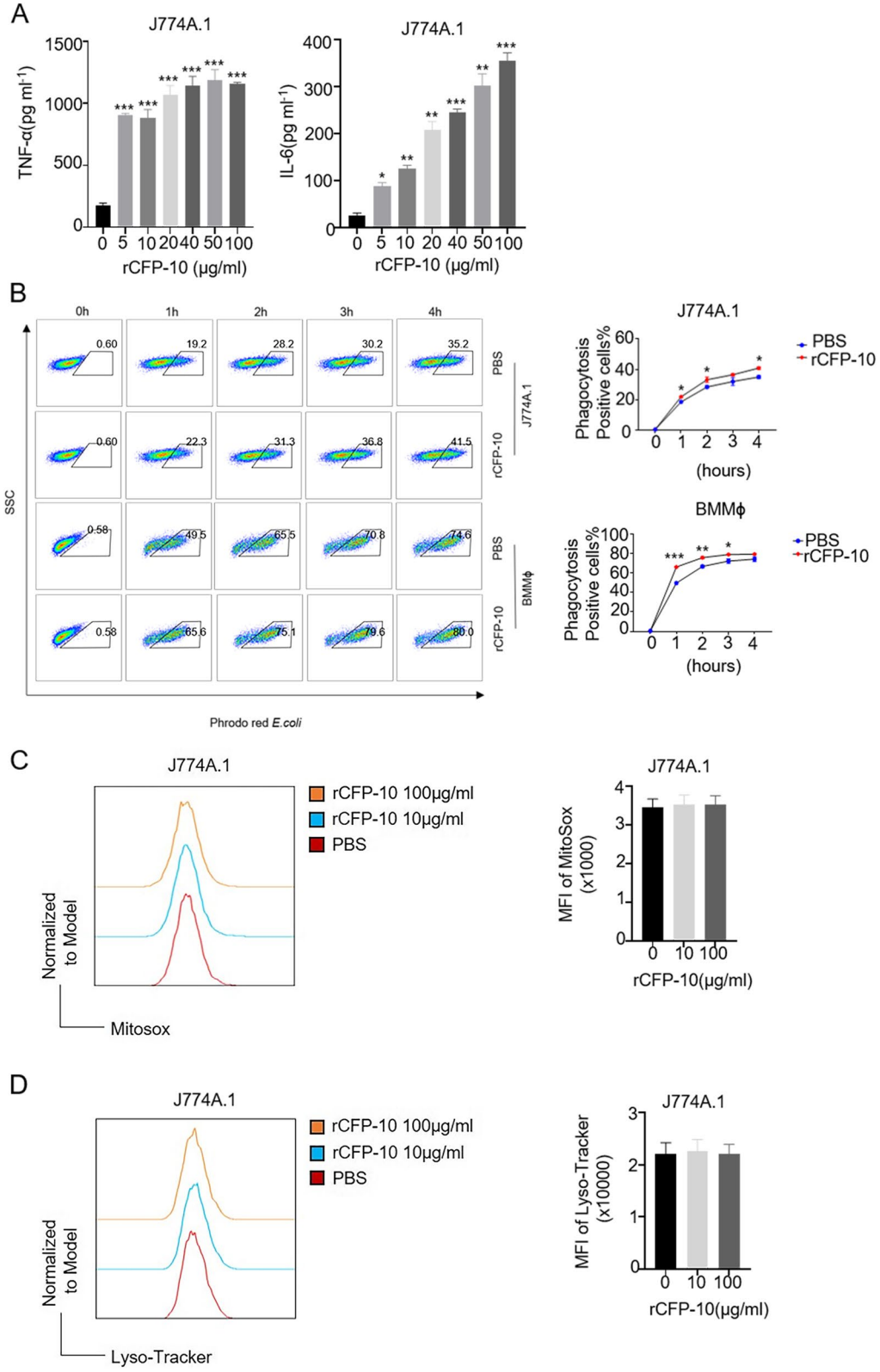

Fig. 3 (See legend on next page.)

(See figure on previous page.)

Fig. 3 rCFP-10 promoted macrophage pro-inflammatory cytokines production and phagocytosis. **A** Production of the pro-inflammatory cytokines TNF-α and IL-6 in J774A.1 cells after treatment with 100 μg/ml of rCFP-10 treatment for 4 h. **B** Phagocytosis of macrophages treated with 100 μg/ml rCFP-10 for 1 h, 2 h, 3 h, and 4 h was determined by Flow Cytometry by staining with Phrodo Red *E.coli*. Left: the representative FACS blots of phagocytosis. Right: the quantification of the phagocytosis efficiency. **C**, **D** Representative histograms show the fluorescence intensity of Mitosox (**C**) and Lyso-Tracker (**D**) in J774A.1 cells with rCFP-10 treatment. Bar figures show the MFI of Mitosox (**C**) and Lyso-Tracker (**D**) in J774A.1 cells with indicated treatments. Data shown are representative of at least three experiments. *: $P < 0.05$; **: $P < 0.01$; ***: $P < 0.001$ was determined by Student *t*-test

for both mTOR1 and mTOR2). As shown in Fig. 4A and Supplement Fig. 2, the rCFP10-induced phosphorylation of Akt in Ser 473 was completely blocked by Torin1 but not by rapamycin, indicating that rCFP10-induced mTORC2 could be suppressed by Torin1. We also observed that rCFP10-enhanced macrophage phagocytosis was significantly reduced after Torin1 treatment (Fig. 4C-E). Thus, these results indicated that rCFP-10 activated macrophage phagocytic capacity partially dependent on mTORC2 activity. Through transcriptome sequencing, we discovered significant changes in genes related to lysosome acidification pathway in J774A.1 cells and BMMϕ treated with rCFP-10 (Fig. 5A and B). As shown in Fig. 5A and B, in comparison to the control group treated with PBS, we found that the expression of the *tmem199* gene was significantly increased in both J774A.1 cells and BMMϕ upon treatment with rCFP-10. The transcription and expression of TMEM199 was also confirmed by RT-PCR and flow cytometry analysis (Fig. 5C-E). Although, the relationship between mTOR signaling and phagosome maturation and lysosome acidification is still not fully understood. We made an intriguing observation that torin1, but not rapamycin, showed a noteworthy increase in the transcriptional level of tmem199 in the presence of rCFP-10 treatment. This finding suggests a potential involvement of mTORC2 signaling in the regulation of rCFP-10-induced tmem199 expression. Tmem199, also known as the transmembrane protein 199, plays a critical role in maintaining lysosomal pH and acidification. Tmem199 is believed to function as a lysosomal membrane protein that interacts with vacuolar ATPase (V-ATPase). Downregulation of the expression of tmem199 can lead to reduced functionality of the V-ATPase complex, resulting in compromised lysosome acidification. These findings indicate that rCFP-10 might have contributed to the *Mtb* intracellular survival by inhibiting lysosome acidification, potentially through the downregulation of tmem199 involved in V-ATPase complex function. The activity of mTORC2 plays a critical role in promoting lysosome acidification by maintaining transcription levels of tmem199 expression. The exact mechanisms by how mTOR signaling affects phagocytosis and lysosome acidification are still being elucidated.

mTORC2 activity was crucial for rCFP10-induced TNFα production and TLR signaling

Studies have shown that CFP-10 can interact with Toll-like receptor 2 (TLR2), a pattern recognition receptor that recognizes microbial components, including those from *Mtb* [28]. The binding of CFP10 to TLR2 also has been shown to activate downstream signaling pathways, including the MyD88-dependent pathway, resulting in the production of pro-inflammatory cytokines, including TNFα [29]. We also observed upregulated expression of the profile of TLRs signaling in rCFP-10 treated J774A.1 cells and BMMϕ (Fig. 6A and B). Moreover, the RT-qPCR results were consistent with the RNASeq data (Fig. 6C-E). The relationship between mTOR signaling and TLR signaling is complex and context-dependent, with interplay and reciprocal regulation occurring between these pathways. In some cases, mTOR signaling can positively regulate TLR signaling. Activation of mTOR has been shown to enhance immune responses downstream of TLRs, leading to increased pro-inflammatory cytokine production [18]. This interaction is important for the initiation and progression of immune responses against pathogens. Conversely, mTOR signaling can also negatively regulate TLR signaling. Under certain conditions, mTOR activation can suppress TLR-mediated inflammation. For example, mTOR inhibition has been found to attenuate TLR-induced pro-inflammatory cytokine production, suggesting a regulatory role of mTOR in controlling excessive immune responses [18, 30]. Moreover, to prevent potential alterations in the expression of the reference gene β-actin due to macrophage activation, which could impact the accuracy of RT-PCR results, we concurrently employed β-tubulin as an additional reference gene. This dual-reference approach ensures the reliability of RT-PCR experimental data in the activated macrophages. Our findings revealed that the expression of *myd88*, *tbk1*, and *tlr2* genes mRNA relative expression was enhanced in J774A.1 cells treated with rCFP-10, and this upregulation was further augmented by treatment with torin1 (Fig. 6C-E, Supplement Fig. 3). However, the expression of TNFα was unexpectedly contradictory to our expectations, as treatment with torin1 led to a further escalation in the levels of TNFα induced by rCFP10 (Fig. 6F). Specifically, the expression level of TNFα decreases, possibly due to competition or inhibition caused by the increased TLR2 signaling with Torin1 treatment. These

results indicated that mTOCR2 activity likely negative regulated rCFP-10-induced TLR2 signaling.

Discussion

Tuberculosis (TB) is a global health problem that causes the highest mortality rate from *Mtb* infection. CFP-10 is one of the secreted proteins of Mycobacterium tuberculosis and has significant importance in the immunological diagnosis of tuberculosis. In this study, we constructed a CFP-10 expression vector and expressed the rCFP-10 protein in *E. coli* BL21 (DE3). The Gram-negative bacilli have endotoxins in their cell walls released upon bacterial disruption and may promote the secretion of inflammatory factors, nitric oxide, and coagulation cascade activation [31]. Thus, the contamination of endotoxin in the recombinant protein expressed by the prokaryotic expression system including in *E. coli* may impact the credibility of the findings. We removed the endotoxin by adsorption resin, which made the rCFP-10 available for use in subsequent in vitro experiments.

Mtb escape from the lysosomal degradation of phagocytes by several mycobacterial proteins [32–34]. We observed that rCFP-10 significantly increased the phagocytic capacity of macrophages in our study in Fig. 3B. In contrast, mtROS level and lysosomal content did not differ significantly with rCFP-10 treatment in Fig. 3C and D, suggesting that rCFP-10 might contribute to *Mtb* invasion and survival in macrophages by enhancing phagocytosis and blocking mtROS production. mtROS are mainly produced by intracellular ROS and are responsible for activating intracellular redox signaling [35]. A recent study by Welin et al. showed that the ESAT-6: CFP-10 complex was recognized by neutrophils. CFP-10, not ESAT-6, was the component that was recognized by neutrophils. In response to CFP-10 stimulation, neutrophils released Ca^{2+} from intracellular stores, resulting in neutrophil chemotaxis and ROS production [36]. Although it was found that both nitric oxide (NO) and ROS levels were decreased in J774A.1 cells following CFP-10 treatment [37, 38], it's important to note that mitochondrial ROS is not equivalent to overall cellular ROS. Additionally, the concentration of CFP-10 used in this study varied from other studies. Together, our results suggested that macrophage mtROS was not possibly involved in rCFP10-induced phagocytosis. Additionally, IL-6 enhances the host immunity against *Mtb* by promoting the secretion of IFN-γ [39, 40].

In the current reports, the mTOR pathway has been shown to play a crucial role in defense against *Mtb* infection. It is known that inhibition of the mTOR pathway can enhance the susceptibility of host defense against invasion by *Mtb*. The mTOR signaling pathway inhibits autophagy; therefore, mTOR inhibitors are a therapeutic strategy that can induce autophagy in *Mtb* infections by targeting the mTOR pathway [41]. To determine whether the phagocytic capacity of macrophages could be affected by rCFP-10 in an mTOR signaling-dependent manner. We used rapamycin or Torin1 in J774A.1 cells and BMMϕ treated with rCFP-10 to investigate the mTOR signaling in rCFP10-induced phagocytosis. Our results proved that the phagocytic capacity of macrophages by rCFP-10 was decreased via inhibition of mTORC2 activity compared to the control in Fig. 4C. Therefore, we have provided evidence that mTORC2 is crucial for promoting macrophage phagocytosis against *Mtb* infection. Nevertheless, the specific role of mTORC2 enhancing phagocytosis mediated by rCFP-10 still needs to be investigated. Additionally, we observed the expression of genes involved in lysosome acidification would be disrupted and the phagocytosis would be enhanced by CFP-10. CFP-10 treatment has been observed to inhibit the expression of tmem199 mRNA. However, this inhibitory effect can be reversed and restored by treatment with torin1. However, the rapamycin treatment could not restore tmem199 expression in rCFP-10 treated J774A.1 cells. This finding suggests that the inhibitory effect of CFP-10 on tmem199 mRNA expression may be mediated through the mTORC2 signaling pathway. In the context of TB, maintaining proper lysosome acidification is critical for the effective elimination of *Mtb* by macrophages. Lysosome acidification creates an acidic environment within the lysosomes, which is necessary for the activity of lysosomal enzymes involved in the degradation of engulfed pathogens. However, dysregulation of mTOR signaling can disrupt this process, leading to impaired lysosome acidification, thereby compromising the ability to degrade and eliminate *Mtb* bacteria.

Both phagocytosis and lysosome acidification play crucial roles in the intracellular clearance of *Mtb* by macrophages [42]. The acidic pH of the phagolysosome is maintained by proton pumps that actively transport hydrogen ions into the compartment. This acidic environment is necessary for the optimal activity of lysosomal enzymes, such as hydrolases, which are responsible for degrading bacterial components and killing *Mtb*. In addition, acidic pH is known to enhance the antimicrobial activity of ROS, which can directly kill *Mtb* by damaging its DNA and other macromolecules [43, 44]. However, *Mtb* has developed sophisticated mechanisms to subvert phagocytosis and evade lysosomal killing. It can interfere with phagosome maturation and inhibit lysosome fusion, thereby avoiding degradation and establishing a replicative niche within macrophage [45–47]. Studies have shown that mTOR signaling can impact phagosome maturation, which is the process by which the phagosome matures into a phagolysosome through fusion with lysosomes. Activation of mTOR has been found to impair

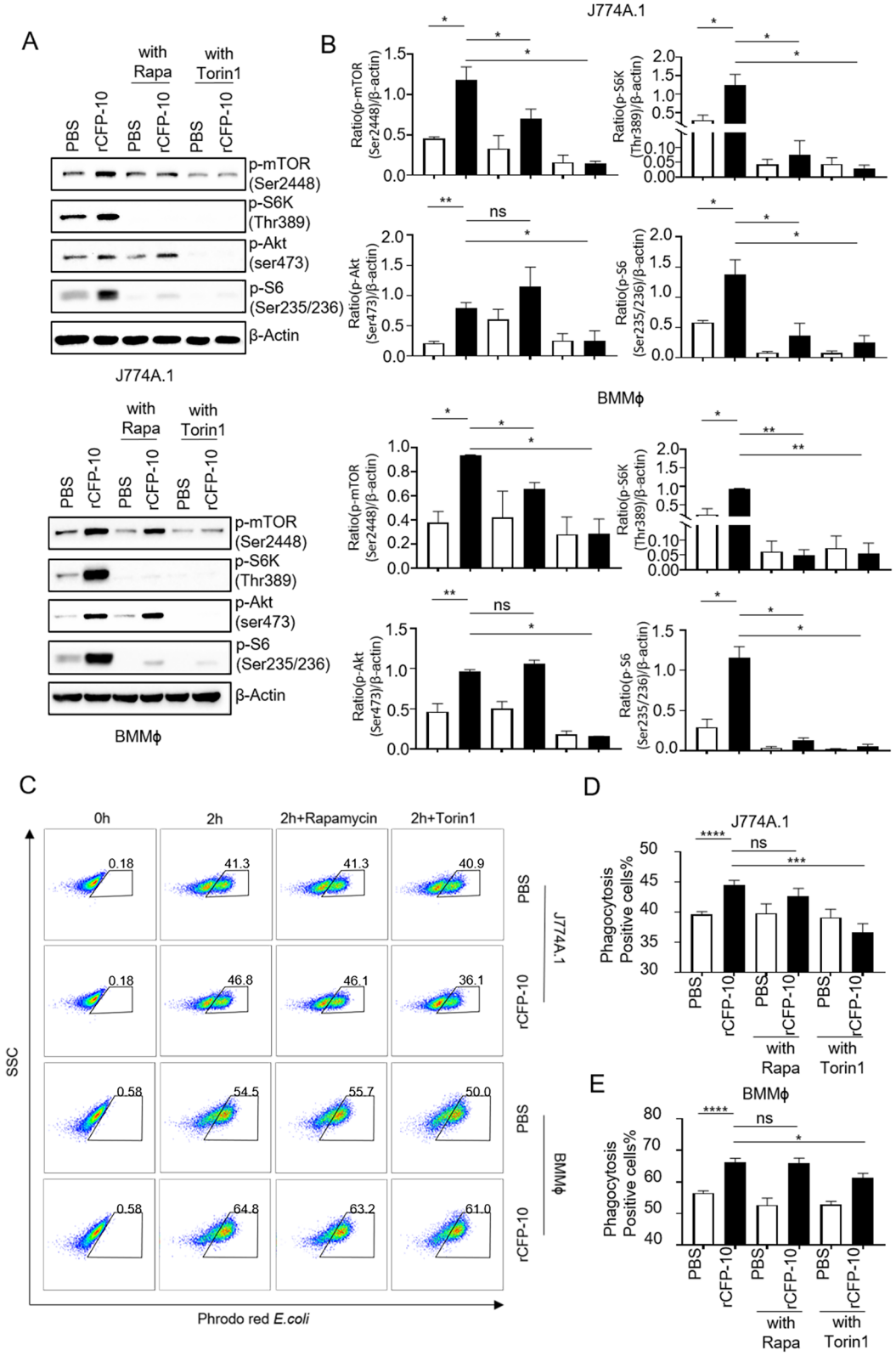

Fig. 4 (See legend on next page.)

(See figure on previous page.)

Fig. 4 The phagocytosis of macrophages by rCFP-10 is dependent on mTORC2 activity. **A** The level of p-mTOR, p-S6 K, p-AKT, p-S6, and β-actin treated with rCFP-10 for 2 h in J774A.1 and BMMϕ were determined by western blot analysis. **B** Bar charts show level of p-mTOR, p-S6 K, p-AKT, p-S6 in J774A.1 cells and BMMϕ with indicated treat-ments. Data shown are representative of at least three experiments. **C** Phagocytosis of J774A.1 cells and BMMϕ treated with 100 μg/ml rCFP-10 for 2 h in the presence of rapamycin and Torin was determined by flow cytometry. **D**,**E** Bar charts show the phagocytosis percentage in J774A.1 cells (**D**) and BMMϕ (**E**) with indicated treatments. Data shown are representative of at least three experiments. *: $P < 0.05$; **: $P < 0.01$; ***: $P < 0.001$; ns = no significant was determined by Student t-test

phagosome maturation in some cases, leading to a delay in the degradation of engulfed pathogens [48, 49].

To sum up, we constructed an expression vector to produce recombinant protein CFP-10 (rCFP-10). We next isolated and purified rCFP-10. We found that rCFP-10 induced both TNF-α and IL-6 production and multiple pathways involved in macrophage activation. Interestingly, the mitochondrial ROS (mtROS) and the lysosomal content of macrophages did not differ significantly. On the other hand, treatment with Torin1, which inhibits both mTORC1 and mTORC2, significantly abolished macrophage phagocytosis. In addition, our observations indicate that the action of rCFP-10 involves the regulation of multiple genes related to the acidification of lysosomes and the signaling pathway involving Toll-like receptor 2 (TLR2) through mTOR signaling. This mechanism potentially plays a role in facilitating the intracellular infection of *Mtb*. In summary, our data suggests that the secreted *Mtb* CFP-10 protein disrupts macrophage functions and inhibits mTORC2 activity. This interference with macrophage function and mTORC2 activity is critical for the regulation of innate immunity against *Mtb* infection. Further exploration in this area also may provide valuable insights into the development of targeted interventions to enhance the immune response against *Mtb* and combat tuberculosis effectively.

Materials and methods

Mice

We purchased 6- to 8-week-old C57BL/6 J mice from the Chinese Academy of Science Shanghai SLAC Laboratory Animal Center. The animal study was reviewed and approved by the Wenzhou Medical University Animal Care and Use Committee (reference number: xmsq2021-0013). All mice were euthanized by carbon dioxide (CO_2) asphyxiation.

Bacterial strains and cell culture

L-929 cells were purchased from the Cell Bank of the Chinese Academy of Science in Shanghai. The J774A.1 mouse monocyte-macrophage cells were purchased from the ATCC Cell Bank and cultured in RPMI1640 containing 10% heat-inactivated fetal bovine serum (Tianhang Bio) with penicillin-streptomycin (50 IU/ml and 50 mg/ml, Beyotime). The GV296 vector was purchased from Shanghai GenePro Technology Co. The *E. coli* BL21 (DE3) is kept in the key laboratory of laboratory medicine, Ministry of Education of China, Wenzhou Medicine University.

Reagents and antibodies

β-Actin (D6 A8) Rabbit mAb, Phospho-mTOR (Ser2448) XP® Rabbit mAb, Phospho-S6 Ribosomal Protei (Ser235/236) (D57.2.2E) XP® Rabbit mAb, Phospho-p70 S6 Kinase (Thr389) (D5U1O) Rabbit mAb, and Phospho-Akt (Ser473) (D9E) XP® Rabbit mAb were purchased from Cell Signaling Technology (CST). 7-Aminoactinomycin D (7-AAD), MitoSOX™ Red mitochondrial superoxide indicator, LysoTracker® Red DND-99, LIVE/DEAD BacLight Bacteria Viability Kits, and pHrodo Red *E. coli* BioParticles were purchased from Invitrogen. HRP-labeled Goat Anti-Rat IgG (H + L), HRP-labeled Goat Anti-Rabbit IgG (H + L), Kanamycin, IPTG, Rapamycin, Torin 1, and His-tag Protein Purification Kit were purchased from Beyotime Biotechnology. Mouse IL-6 Elisa kit and Mouse TNFα Elisa kit were purchased from Shanghai Dakowei Biotechnology Co. DEAE Focurose 6 FF was purchased from Wuhan Huiyan Biotechnology Co. EtEraser High-Performance Endotoxin Removal Kit and Tachypleus amebocyte lysate were purchased from Xiamen Bioendo Technology Co.

Primers

The gene encoding CFP-10 along with its promoter was amplified by PCR using forward (5'-AGCAAATGGGT CGCGGATCCATGGCAGAGATGAAGACCGATG-3') and reverse (5'-GCGGCCGCAAGCTTGTCGACTTAC TTGTACAGCTCGTCCATGC-3') primers. The restriction sites for primers were BamHI and SalI. The primers for RT-PCR were listed in Table 1. The primers were synthesized by Shanghai Gikai Gene Technology Co.

rCFP-10 cloned to GV296 vector

The gene encoding CFP-10 of *M. tuberculosis* was amplified by PCR from genomic DNA. The reaction conditions were as follows: 98 °C for 5 min, 98 °C for 10 s, 55 °C for 10 s, and 72 °C for 90 s for 30 cycles; this was followed by 72 °C for 8 min and maintained at 4 °C for preservation. Then the PCR product was eluted from an agarose gel, digested with BamHI and SalI, and ligated into the GV296 vector with the ClonExpressTM II One Step Cloning Kit (Vazyme Biotech Co., Ltd). The recombinant plasmids were transformed into *E. col* BL21 bacterial

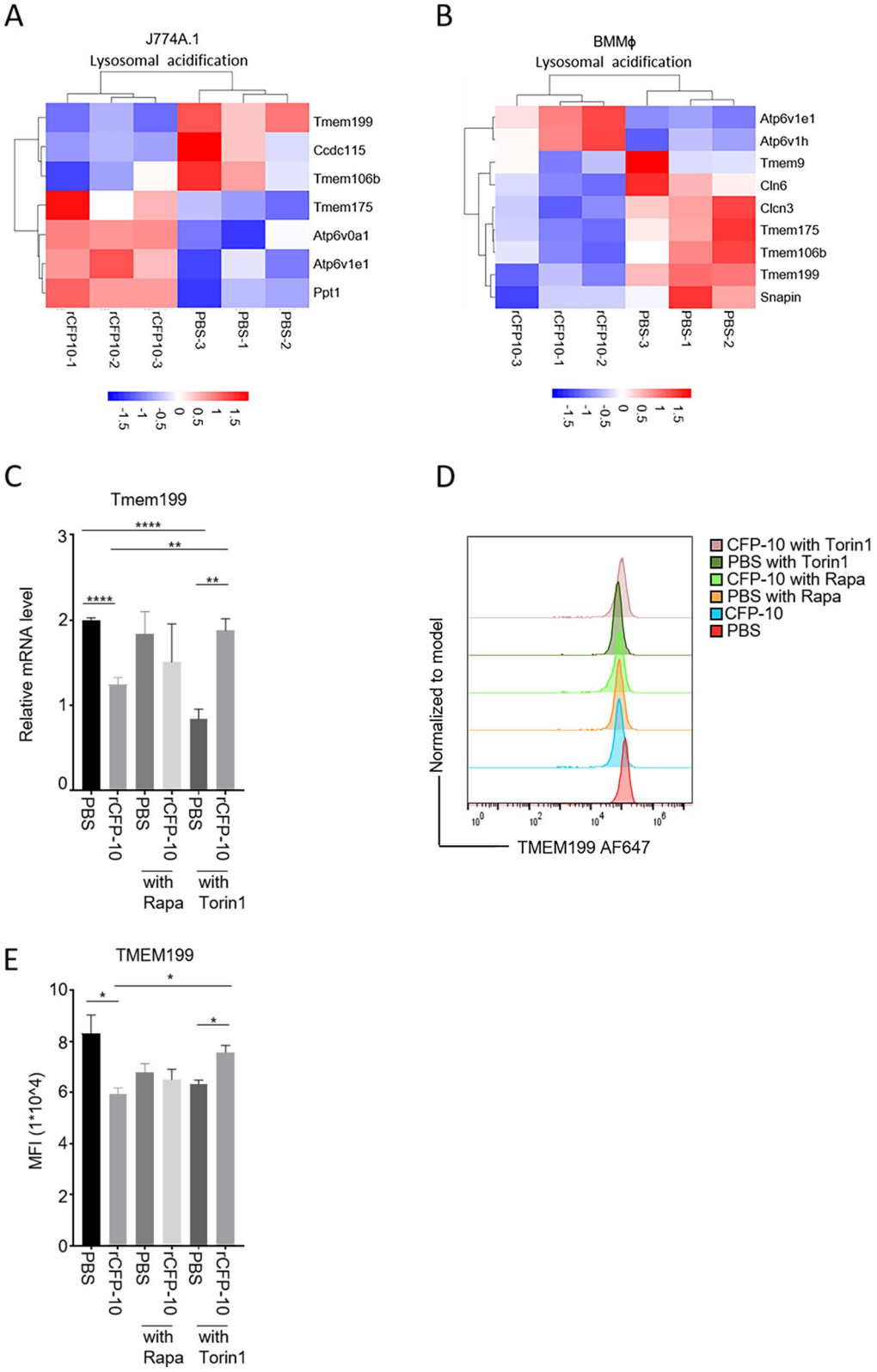

Fig. 5 (See legend on next page.)

(See figure on previous page.)

Fig. 5 The expression level of tmem199, which is involved in lysosome acidification, in macrophages treated with rCFP-10 is reliant on the activity of mTORC2. **A**, **B** Heapmap of transcriptional profiles of J774A.1 cells and BMMϕ with or without rCFP-10 treatment (PBS: $n = 3$; rCFP-10: $n = 3$). Gene expressions are presented as log2 fluorescence intensity centered and scaled (blue and red keys) grouped according to the product functions. **C** Transcrption of Tmem199 was relative to β-actin in the J774A.1 cells after treatment with 100 μg/ml of rCFP-10 treatment for 2 h in the presence or absence of rapamycin and Torin1 pretreatment. **D** Expression of TMEM199 in the J774A.1 cells after treatment with 100 μg/ml of rCFP-10 treatment for 2 h in the presence or absence of rapamycin and Torin1 pretreatment determined by flow cytometry. **E** Bar charts show level of TMEM199 in the J774A.1 cells after treatment with 100 μg/ml of rCFP-10 treatment for 2 h in the presence or absence of rapamycin and Torin1 pretreatment. *: $P < 0.05$; **: $P < 0.01$; ***: $P < 0.001$; ns = no significant was determined by Student *t*-test

cells (DE3) and subjected to sequencing (Shanghai Gikai Gene Technology Co.).

Induced expression and purification of rCFP-10

The above-mentioned *E. coli* BL21 transformant was grown in Luria-Bertani medium with 50 μg/mL kanamycin (Beyotime) at 37 °C. Five-milliliter starter cultures were grown to stationary phase overnight with shaking in Luria-Bertani broth with 50 μg/mL Kanamycin (Beyotime). These were used to inoculate 1 L of LB media to grow in shaking flasks at 37 °C. Once cultures reached an OD600 between 0.5 and 0.8, recombinant protein CFP-10 production was induced using 800 μM IPTG (Beyotime). Cultures were grown for 6 h, with shaking at 25 °C. Bacteria were then pelleted at 4,000× rpm for 10 min and resuspended in lysis buffer. The bacteria were purified by affinity chromatography based on the instructions of the His-tag Protein Purification Kit (P2226, Beyotime, China). Recombinant proteins were subsequently concentrated with Amicon Ultra-15 filters. Filtration was performed according to the Millipore protocols provided with the filters. Next, DEAE columns were washed with 10 column volumes (CVs) of double distilled water and were equilibrated using 10 CVs of 0.02 M Tris-HCl (pH 8.2). Following, the recombinant proteins were loaded onto DEAE columns by gravity. Samples were then washed with 10 CVs 0.02 M Tris-HCl (pH 8.2) and then eluted with a linear gradient from 6 to 13% of an elution buffer containing 0.02 M Tris-HCl (pH 8.2) and 1 M NaCl. Fractions were collected and monitored for recombinant protein elution and purity by SDS/PAGE followed by Coomassie Blue stain. The recombinant proteins were aliquoted and frozen for subsequent use. According to the instruction manual, the endotoxin was removed with the EtEraser Endotoxin Removal Kit (Xiamen Bioendo Technology Co., Ltd.). The endotoxin level of the protein extract did not exceed 1.0 EU/ml and was detected with the horseshoe crab reagents (Xiamen Bioendo Technology Co., Ltd.).

RNA sequencing

J774A.1 cells and BMMϕs treated with 1 h 100ug/ml rCFP-10 or PBS were used for RNA sequencing. Briefly, the cells were lysed in TRIzol and subjected to Annoroad Co. for RNA extraction, sequencing, and transcriptome profile analysis. The significantly differentially expressed genes were identified when we compared the normalized reads count between CFP-10 and PBS groups with $p < 0.05$ and |Log2 FoldChange| > 0.263. The significance of the gene ontology term enrichment was estimated using Fisher's Exact Test (p value).

Quantitative PCR analysis

The J774A.1 cells were induced by 100 μg/ml rCFP-10 for 2 h. Total RNA was extracted with TRIzol (Omega Bio-Tek), and reverse transcription was performed using PrimeScript Reverse Transcriptase (RR037 A, Takara Bio) according to the manufacturer's instructions. Real-time qPCR was conducted as previously described [19]. The primers sequences used are provided in Table 1. To determine the relative induction of TLR signaling mRNA, the mRNA expression was normalized with β-actin and calculated using the $2^{-\triangle\triangle CT}$ method.

Acquisition of bone Marrow-Derived macrophages (BMMϕs)

The bone marrow cells were isolated from femurs and tibiae and cultured with a 10% L-929 cell culture medium, as described previously [50]. Bone marrow cells were cultured with 1640 medium (Gibco) containing 10% (v/v) FBS and 15% (v/v) L929 conditional medium for seven days to obtain bone marrow-derived macrophages.

rCFP-10 effect on bone Marrow-Derived macrophages (BMMϕs) and J774A.1 cells in vitro

A total of 1×10^6 or 0.5×10^6 BMMϕ from C57BL/6 J (WT) or J774A.1 cells was equally seeded in six- or twelve-well plates and cultured at 37 °C overnight. We then added rCFP-10 at the corresponding concentration to the medium for the appropriate time. The supernatant was collected at the indicated time for cytokine quantification. The affected cells were used for flow cytometry analysis and Western blot analysis.

Western blot analysis

Cell lysate preparation and Western blot analysis followed the previous protocol [19]. Briefly, macrophages were cultured in RPMI 1640 medium with 10% FBS in six-well plates. Cells were treated with 100ug/ml rCFP-10 for 2 h. Cells were washed twice in cold PBS, then were lysed in RIPA buffer (Beyotime Bio) with protease and phosphatase inhibitor cocktails

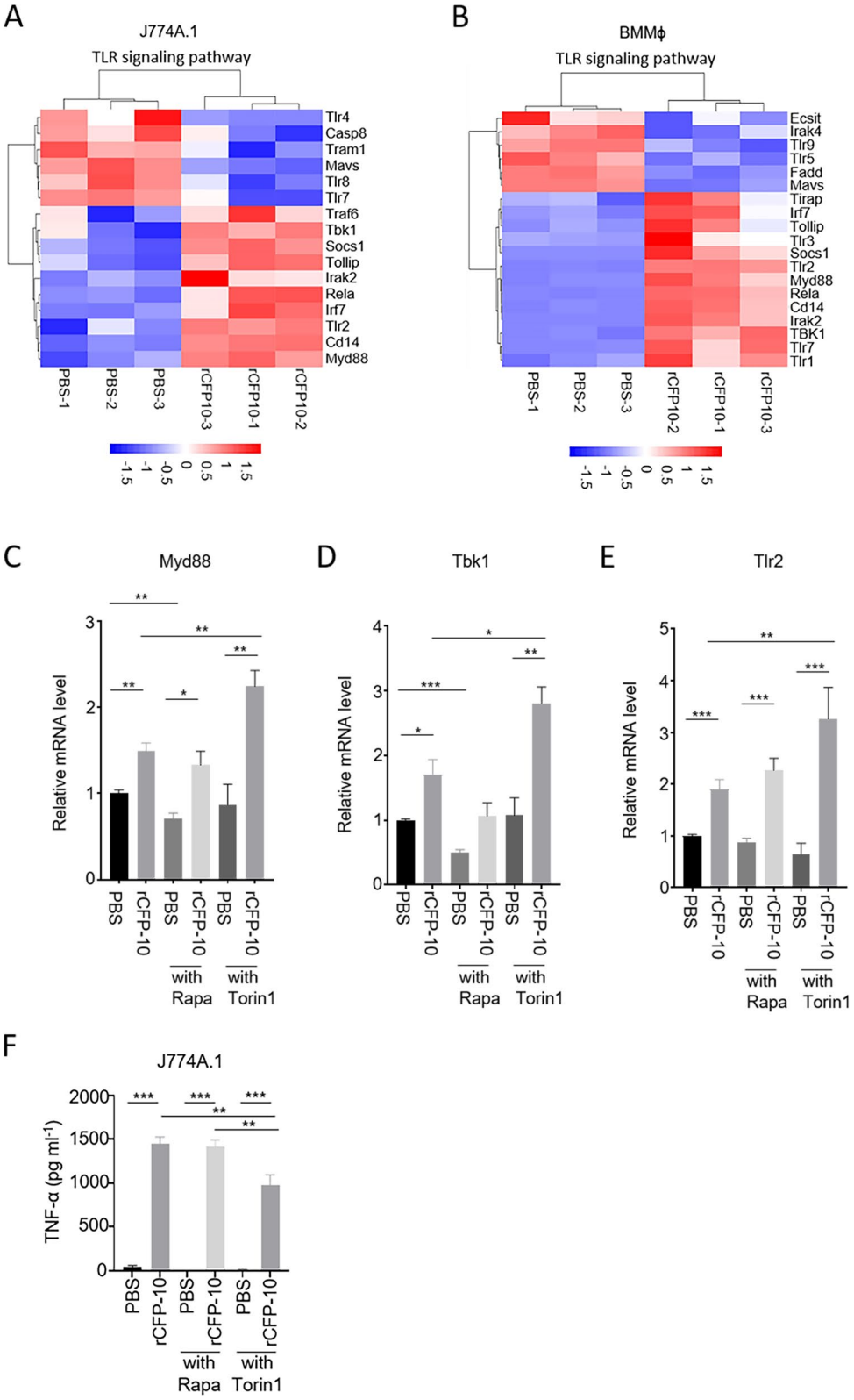

Fig. 6 (See legend on next page.)

(See figure on previous page.)

Fig. 6 mTORC2 activity was crucial for the expression of genes involved in TLR signaling. **A**, **B** Heapmap of transcriptional profiles of J774A.1 cells and BMMϕ with or without rCFP-10 treatment (PBS: $n = 3$; rCFP-10: $n = 3$). Gene expressions are presented as log2 fluorescence intensity centered and scaled (blue and red keys) grouped according to the product functions. **A** The TLR signaling pathway is expressed in the J774A.1 cell. **B** The TLR signaling pathway is expressed in the BMMϕ. **C-E** Transcription of Myd88, TBK1, TLR2 was relative to β-actin in J774A.1 cells after treatment with 100 μg/ml of rCFP-10 treatment for 2 h in the presence or absence of rapamycin and Torin1 pretreatment. **F** Production of the pro-inflammatory cytokine TNF-α in the supernatant of J774A.1 cells after treatment with 100 μg/ml of rCFP-10 treatment for 4 h in the presence or absence of rapamycin and Torin1 pretreatment. *: $P < 0.05$; **: $P < 0.01$; ***: $P < 0.001$; ns = no significant was determined by Student *t*-test

(Sigma) for 15 min at 4 °C. Protein concentration was determined by Bradford assay. Protein samples were analyzed by SDS–PAGE gel and transferred to PVDF membrane. The membrane was blocked with 5% non-fat dried milk in TBST (100 mM Tris–HCl pH 7.5, 150 mM NaCl, 0.05% Tween20) for 1 h, then incubated with indicated primary antibodies overnight on a shaker at 4 °C. The appropriate HRP-coupled secondary antibody was then added and was detected through ECL chemiluminescence (BioRad). β-actin was used as a protein loading control.

Macrophage phagocytosis

Briefly, macrophages were cultured in RPMI 1640 medium with 10% FBS in twelve-well plates. Cells were treated with 100 μg/ml rCFP-10 for 2 h. For the macrophage phagocytosis experiment, cells were resuspended in 1 mg/ml pHrodo Red *E. coli* bioparticles (Thermo Fisher Scientific) and incubated at 37 °C for 0 h, 1 h, 2 h, 3 h, and 4 h. Cells were washed and stained for flow cytometry. Macrophages that were PE-high were considered to be phagocytosing.

Measurement of mitochondrial superoxide production and lysosomal content

Mitochondria-targeted MitoSOX™ Red fluorogenic dye (Thermo Fisher Scientific, Rockford, IL, USA) and LysoTracker1 Red DND-99 (Thermo Fisher Scientific, Rockford, IL, USA) were used to measure mitochondrial superoxide accumulation and lysosomal content according to the manufacturer's instructions. Briefly, cells were seeded in 12-well plates for 1 h and then were treated with 100 μg/ml rCFP-10 for the appropriate time. Cells were incubated for 30 min at 37 °C in 0.2 mL of measurement buffer containing 0.2uL MitoSOX™ Red. Then, the cells were washed twice with PBS. MitoSOX™ fluorescence was measured by flow cytometry. The lysosome content detection also followed the above steps.

Table 1 Primer sequences used for quantitative PCR analysis

Primer	Sequence (5′–3′)
Tmem199 F	AGTGATAATGCCACGGGACC
Tmem199 R	CCTCACTTGCTTTCCCAGGT
TLR2 F	ACCAAGATCCAGAAGAGCCA
TLR2 R	CATCACCGGTCAGAAAACAA
Myd88 F	CTTAACGTGGGAGTGAGGC
Myd88 R	ACAAACTGCGAGTGGGGT
TBK1 F	GAAGAAGTACGGGGCTACCG
TBK1 R	GTGCCTGAAGACCCTGAGAA
β-actin F	GCTGTGCTATGTTGCTCTAG
β-actin R	CGCTCGTTGCCAATAGTG
β-tubulin F	GGAAGAGGATTTCGGAGAGG
β- tubulin R	GGACAGAGGCAGCAGAAAGA

F Forward primer, *R* Reverse primer

Intracellular TMEM199 detection

Macrophages were cultured in RPMI 1640 medium with 10% FBS in twelve-well plates. Cells were treated with 100 μg/ml rCFP-10 for 2 h. For intracellular staining, cells were incubated for 15 min on ice with Cytofix/Cytoperm Fixation/Permeabilization solution (BD Biosciences). Intracellular proteins were stained at 25 °C for 1 h with Rabbit anti-mouse TMEM199 (DF13885, Affinity Biosciences) diluted 1:50 (ab150077, Abcam) and Alexa Fluor® 647-conjugated Goat anti rabbit IgG (Alexa Fluor®488, Abcam) at 1/500 dilution in Perm/Wash Buffer. Cells were washed and stained for flow cytometry.

Cytokine production assay

Cytokine concentration was determined using ELISA kits for TNFα and IL-6 (Diatek, Shanghai, China). We purchased IL-6 and TNFα Elisa Kit from Shanghai Dakowei Biotechnology Co to measure IL-6 and TNFα production in the supernatant. Briefly, the supernatant from cultured cells with indicated treatment was collected and centrifuged at 4 °C 3,000 rpm per 10 min, and then was analyzed by following the manufacturer's instructions.

Cell viability assay

Cells were added to each well at a density of 5×10^3/mL and cultured for 1 h at 37 ℃, then were added rCFP-10 at the corresponding concentration for the appropriate time. 10uL of Cell Counting Kit-8 (CCK8) solution (Dojindo) was added to the medium in 96-well plates at 37 ℃ for 2 h. The plates were then read using a standard plate reader with a reference wavelength of 450 nm.

Statistical analysis

Data were presented as mean ± SEM and analyzed for statistical differences using the Prism 6.01/GraphPad software. Statistical significance was analyzed using the Student t-test. *P*-values less than 0.05 were considered significant.

Supplementary Information

The online version contains supplementary material available at https://doi.org/10.1186/s12865-025-00715-6.

Supplementary Material 1.

Acknowledgements
We thank the flow cytometry core facility of Wenzhou Medical University for their service.

Authors' contributions
D.X., L.W., and Y.L. conceived the work. D.X., L.T., Y.W., X.H., L.W., L.M., Y.J., X.S., X.W., and M.Z. analyzed data. L.T., Y.W., Y.L., X.H., and L.W. wrote the manuscript. Y.W., X.H., L.M., L.W., and Y.J. performed experiments. D.X. supervised the work and wrote the manuscript. All authors read and approved the final manuscript.

Funding
This work was supported by the Natural Science Foundation of Zhejiang Province (LY22H190002), the Medical Health Science and Technology Project of Zhejiang Provincial Health Commission (2022RC045), Wenzhou Science and Technology Plan Project (Y2020217), the Zhejiang Provincial Science and Technology Innovation Program (New Young Talent Program) for College Students (2021R413031), the National Key Research and Development Program (2021YFC2300300), and the Youth Independent Innovation Science Foundation of PLA General Hospital (22QNFC118).

Data availability
The RNASeq datasets generated and/or analyzed during the current study are available in the NCBI BioProject database repository with the accession number PRJNA922436 (https://www.ncbi.nlm.nih.gov/bioproject/922436).

Declarations

Ethics approval and consent to participate
The animal study was reviewed and approved by the Wenzhou Medical University Animal Care and Use Committee (reference number: xmsq2021-0013). All animal experiments were ethically performed in accordance with the relevant guidelines and regulations. All mice were euthanized by carbon dioxide (CO_2) asphyxiation.

Consent for publication
Not applicable.

Competing interests
The authors declare no competing interests.

Received: 29 December 2022 / Accepted: 24 April 2025
Published online: 09 May 2025

References

1. MacNeil A, Glaziou P, Sismanidis C, Date A, Maloney S, Floyd K. Global epidemiology of tuberculosis and progress toward meeting global Targets - Worldwide, 2018. MMWR Morb Mortal Wkly Rep. 2020;69(11):281–5.
2. Paulson T. Epidemiology: A mortal foe. Nature. 2013;502(7470):S2–3.
3. Abdallah AM, van Gey NC, Champion PA, Cox J, Luirink J, Vandenbroucke-Grauls CM, Appelmelk BJ, Bitter W. Type VII secretion–mycobacteria show the way. Nat Rev Microbiol. 2007;5(11):883–91.
4. Gröschel MI, Sayes F, Simeone R, Majlessi L, Brosch R. ESX secretion systems: mycobacterial evolution to counter host immunity. Nat Rev Microbiol. 2016;14(11):677–91.
5. Renshaw PS, Lightbody KL, Veverka V, Muskett FW, Kelly G, Frenkiel TA, Gordon SV, Hewinson RG, Burke B, Norman J, et al. Structure and function of the complex formed by the tuberculosis virulence factors CFP-10 and ESAT-6. EMBO J. 2005;24(14):2491–8.
6. Berthet FX, Rasmussen PB, Rosenkrands I, Andersen P, Gicquel B. A Mycobacterium tuberculosis Operon encoding ESAT-6 and a novel low-molecular-mass culture filtrate protein (CFP-10). Microbiol (Reading). 1998;144(Pt 11):3195–203.
7. Sørensen AL, Nagai S, Houen G, Andersen P, Andersen AB. Purification and characterization of a low-molecular-mass T-cell antigen secreted by Mycobacterium tuberculosis. Infect Immun. 1995;63(5):1710–7.
8. Fu B, Xue W, Zhang H, Zhang R, Feldman K, Zhao Q, Zhang S, Shi L, Pavani KC, Nian W et al. MicroRNA-325-3p facilitates immune escape of mycobacterium tuberculosis through targeting LNX1 via NEK6 accumulation to promote anti-apoptotic STAT3 signaling. mBio. 2020;11(3):e00557–20.
9. Bickett TE, Karam SD. Tuberculosis-Cancer parallels in immune response regulation. Int J Mol Sci. 2020;21(17):6136.
10. Jamwal SV, Mehrotra P, Singh A, Siddiqui Z, Basu A, Rao KV. Mycobacterial escape from macrophage phagosomes to the cytoplasm represents an alternate adaptation mechanism. Sci Rep. 2016;6:23089.
11. Chen Z, Wang T, Liu Z, Zhang G, Wang J, Feng S, Liang J. Inhibition of autophagy by MiR-30A induced by mycobacteria tuberculosis as a possible mechanism of immune escape in human macrophages. Jpn J Infect Dis. 2015;68(5):420–4.
12. Wong D, Li W, Chao JD, Zhou P, Narula G, Tsui C, Ko M, Xie J, Martinez-Frailes C, Av-Gay Y. Protein tyrosine kinase, PtkA, is required for Mycobacterium tuberculosis growth in macrophages. Sci Rep. 2018;8(1):155.
13. Wei S, Wang D, Li H, Bi L, Deng J, Zhu G, Zhang J, Li C, Li M, Fang Y, et al. Fatty acylcoa synthetase FadD13 regulates Proinflammatory cytokine secretion dependent on the NF-κB signalling pathway by binding to eEF1A1. Cell Microbiol. 2019;21(12):e13090.
14. Chai Q, Wang L, Liu CH, Ge B. New insights into the evasion of host innate immunity by Mycobacterium tuberculosis. Cell Mol Immunol. 2020;17(9):901–13.
15. Villarreal-Ramos B, Berg S, Whelan A, Holbert S, Carreras F, Salguero FJ, Khatri BL, Malone K, Rue-Albrecht K, Shaughnessy R, et al. Experimental infection of cattle with Mycobacterium tuberculosis isolates shows the Attenuation of the human tubercle bacillus for cattle. Sci Rep. 2018;8(1):894.
16. Chandra P, He L, Zimmerman M, Yang G, Köster S, Ouimet M, Wang H, Moore KJ, Dartois V, Schilling JD, et al. Inhibition of fatty acid oxidation promotes macrophage control of Mycobacterium tuberculosis. mBio. 2020;11(4):e01139–20.
17. Covarrubias AJ, Aksoylar HI, Horng T. Control of macrophage metabolism and activation by mTOR and Akt signaling. Semin Immunol. 2015;27(4):286–96.
18. Weichhart T, Hengstschläger M, Linke M. Regulation of innate immune cell function by mTOR. Nat Rev Immunol. 2015;15(10):599–614.
19. Xie DL, Wu J, Lou YL, Zhong XP. Tumor suppressor TSC1 is critical for T-cell anergy. Proc Natl Acad Sci U S A. 2012;109(35):14152–7.
20. Saunders BM, Frank AA, Orme IM, Cooper AM. Interleukin-6 induces early gamma interferon production in the infected lung but is not required for generation of specific immunity to Mycobacterium tuberculosisinfection. Infect Immun. 2000;68(6):3322–6.
21. Rothfuchs AG, Bafica A, Feng CG, Egen JG, Williams DL, Brown GD, Sher A. Dectin-1 interaction with Mycobacterium tuberculosis leads to enhanced IL-12p40 production by splenic dendritic cells. J Immunol (Baltimore, Md: 1950). 2007;179(6):3463–71.
22. Saviola B. "All stressed out: Mycobacterial responses to stress". In: Mendez-Vilas A, editor. Current Research, Technology, and Education Topics in Applied Microbiology and Microbial Biotechnology. Microbiology Book Series Edition, (Formatex Research Center). 2010. p. 545–49.
23. Colangeli R, Haq A, Arcus VL, Summers E, Magliozzo RS, McBride A, Mitra AK, Radjainia M, Khajo A, Jacobs WR Jr. The multifunctional histone-like protein Lsr2 protects mycobacteria against reactive oxygen intermediates. Proc Natl Acad Sci U S A. 2009;106(11):4414–8.
24. Sica A, Erreni M, Allavena P, Porta C. Macrophage polarization in pathology. Cell Mol Life Sci Cmls. 2015;72(21):4111–26.
25. Wang X, Li M, Gao Y, Gao J, Yang W, Liang H, Ji Q, Li Y, Liu H, Huang J, et al. Rheb1-mTORC1 maintains macrophage differentiation and phagocytosis in mice. Exp Cell Res. 2016;344(2):219–28.
26. Wang Z, Zhou S, Sun C, Lei T, Peng J, Li W, Ding P, Lu J, Zhao Y. Interferon-γ inhibits nonopsonized phagocytosis of macrophages via an mTORC1-c/EBPβ pathway. J Innate Immun. 2015;7(2):165–76.
27. Farina M, Avila DS, da Rocha JB, Aschner M. Metals, oxidative stress and neurodegeneration: a focus on iron, manganese and mercury. Neurochem Int. 2013;62(5):575–94.
28. Saraav I, Singh S, Sharma S. Outcome of Mycobacterium tuberculosis and Toll-like receptor interaction: immune response or immune evasion? Immunol Cell Biol. 2014;92(9):741–6.

29. Kleinnijenhuis J, Oosting M, Joosten LA, Netea MG, Van Crevel R. Innate immune recognition of Mycobacterium tuberculosis. Clin Dev Immunol. 2011;2011:405310.
30. Anwar MA, Basith S, Choi S. Negative regulatory approaches to the Attenuation of Toll-like receptor signaling. Exp Mol Med. 2013;45(2):e11.
31. Anspach FB. Endotoxin removal by affinity sorbents. J Biochem Biophys Methods. 2001;49(1–3):665–81.
32. Bosedasgupta S, Pieters J. Striking the right balance determines TB or not TB. Front Immunol. 2014;5:455.
33. Pieters J. Mycobacterium tuberculosis and the macrophage: maintaining a balance. Cell Host Microbe. 2008;3(6):399–407.
34. Rohde K, Yates RM, Purdy GE, Russell DG. Mycobacterium tuberculosis and the environment within the phagosome. Immunol Rev. 2007;219:37–54.
35. Wang SM, Lim SW, Wang YH, Lin HY, Lai MD, Ko CY, Wang JM. Astrocytic CCAAT/Enhancer-binding protein delta contributes to reactive oxygen species formation in neuroinflammation. Redox Biol. 2018;16:104–12.
36. Welin A, Björnsdottir H, Winther M, Christenson K, Oprea T, Karlsson A, Forsman H, Dahlgren C, Bylund J. CFP-10 from Mycobacterium tuberculosis selectively activates human neutrophils through a pertussis toxin-sensitive chemotactic receptor. Infect Immun. 2015;83(1):205–13.
37. Trajkovic V, Singh G, Singh B, Singh S, Sharma P. Effect of Mycobacterium tuberculosis-specific 10-kilodalton antigen on macrophage release of tumor necrosis factor alpha and nitric oxide. Infect Immun. 2002;70(12):6558–66.
38. Basu SK, Kumar D, Singh DK, Ganguly N, Siddiqui Z, Rao KV, Sharma P. Mycobacterium tuberculosis secreted antigen (MTSA-10) modulates macrophage function by redox regulation of phosphatases. FEBS J. 2006;273(24):5517–34.
39. Guirado E, Schlesinger LS. Modeling the Mycobacterium tuberculosis Granuloma - the critical battlefield in host immunity and disease. Front Immunol. 2013;4:98.
40. Barry CE 3rd, Boshoff HI, Dartois V, Dick T, Ehrt S, Flynn J, Schnappinger D, Wilkinson RJ, Young D. The spectrum of latent tuberculosis: rethinking the biology and intervention strategies. Nat Rev Microbiol. 2009;7(12):845–55.
41. Harrison DE, Strong R, Sharp ZD, Nelson JF, Astle CM, Flurkey K, Nadon NL, Wilkinson JE, Frenkel K, Carter CS, et al. Rapamycin fed late in life extends lifespan in genetically heterogeneous mice. Nature. 2009;460(7253):392–5.
42. Weiss G, Schaible UE. Macrophage defense mechanisms against intracellular bacteria. Immunol Rev. 2015;264(1):182–203.
43. Mindell JA. Lysosomal acidification mechanisms. Annu Rev Physiol. 2012;74:69–86.
44. Baker JJ, Dechow SJ, Abramovitch RB. Acid fasting: modulation of Mycobacterium tuberculosis metabolism at acidic pH. Trends Microbiol. 2019;27(11):942–53.
45. Zhai W, Wu F, Zhang Y, Fu Y, Liu Z. The immune escape mechanisms of Mycobacterium Tuberculosis. Int J Mol Sci. 2019;20(2):340.
46. Melly G, Purdy GE. MmpL proteins in physiology and pathogenesis of M. tuberculosis. Microorganisms. 2019;7(3):70.
47. Gupta A, Kaul A, Tsolaki AG, Kishore U, Bhakta S. Mycobacterium tuberculosis: immune evasion, latency and reactivation. Immunobiology. 2012;217(3):363–74.
48. Noda T, Ohsumi Y. Tor, a phosphatidylinositol kinase homologue, controls autophagy in yeast. J Biol Chem. 1998;273(7):3963–6.
49. Monteith AJ, Vincent HA, Kang S, Li P, Claiborne TM, Rajfur Z, Jacobson K, Moorman NJ, Vilen BJ. mTORC2 activity disrupts lysosome acidification in systemic lupus erythematosus by impairing Caspase-1 cleavage of Rab39a. J Immunol (Baltimore Md: 1950). 2018;201(2):371–82.
50. Pan H, O'Brien TF, Zhang P, Zhong XP. The role of tuberous sclerosis complex 1 in regulating innate immunity. J Immunol (Baltimore Md: 1950). 2012;188(8):3658–66.

Publisher's Note